FACTORS CONTROLLING THE RELEASE AND ATTENUATION OF CONTAMINANTS IN A SULFIDIC TAILINGS IMPOUNDMENT[1]

by

B. M. Stewart,[2] R. H. Lambeth,[2] and B. C. Williams[3]

Abstract. Researchers at the U.S. Bureau of Mines have been collecting physical property data and monitoring ground water at a 10-hectare (ha), 6-meter (m)-deep pyritic tailings impoundment in northeastern Washington. The purpose is to investigate metal release, metal transport, and attenuation mechanisms in, below, and downgradient of the impoundment. Physical and chemical characteristics and the hydrodynamic processes at the site control these mechanisms. Some of these characteristics include very low horizontal hydraulic gradients through the tailings, increases in the percentage of fine particles with depth, sporadic development of hardpan layers in the vadose zone resulting from secondary mineral precipitation, the potentially significant neutralizing capacity of the sediments below the tailings, and the potential for mixing of tailings leachate with ground water.

A detailed geochemical analysis of the site aided in characterizing the geochemical changes and reactions that occurred along the groundwater flow path through the tailings and downgradient of the impoundment. Results of the analysis indicate that as contaminated pore water leaves the tailings, either oxidation or neutralization and an increase in pH control attenuation. However, farther downgradient oxidation may be controlling attenuation.

Additional Key Words: tailings physical properties, dissolved metals, neutralization, hydrogeology, hydrodynamics, geochemical modeling.

Introduction

The U.S. Bureau of Mines is conducting long-term research into the generation, mobilization, and fate of heavy metals and other contaminants in tailings from milling operations. The goal is to identify the underlying mechanisms that cause contamination, investigate site-specific controls of contamination, and use this information to reduce contamination in a cost-effective manner.

This paper describes research at a mine waste site in northern Washington. It includes site characterization and analytical results from water quality data collected from the unsaturated and saturated tailings, the saturated silty sediments below the tailings, and an unconsolidated
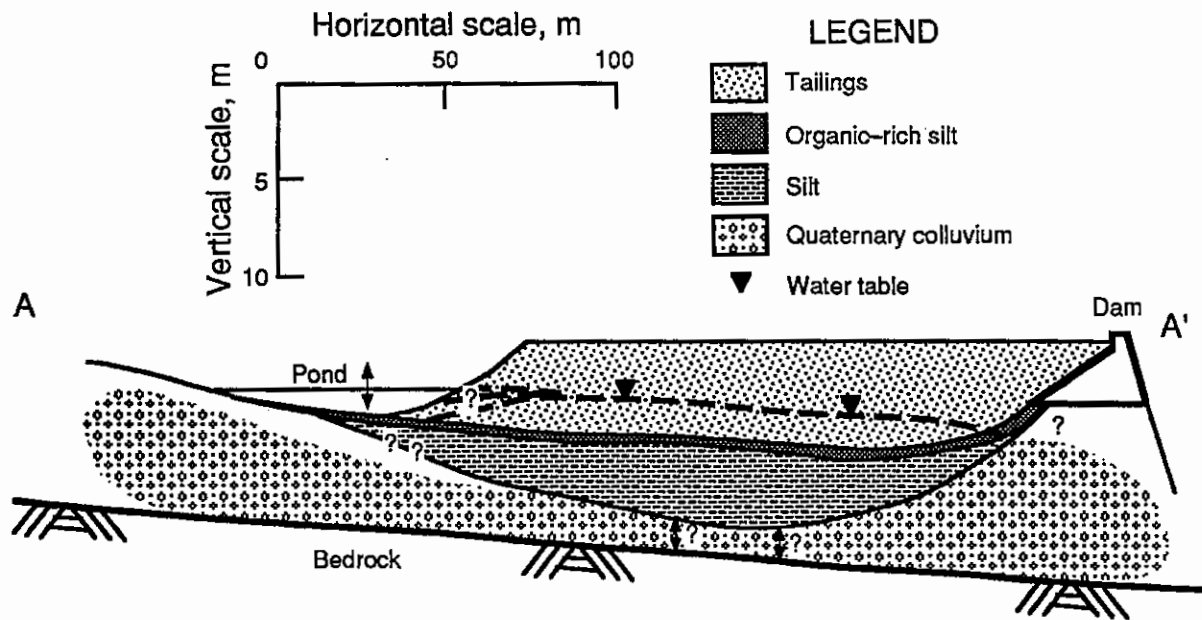
Figure 1. Cross section of tailings impoundment and stratigraphy below impoundment.

gravel aquifer. The primary objectives of the investigation are to determine (1) the influence of the partially saturated zone on acid production and the leaching and transport of dissolved metals from the waste and (2) how site-specific geological, physical, and hydrochemical properties of the waste and host environment either maintain or attenuate transport of dissolved metals and other contaminants in ground water.

Site Description

The site chosen for this research was an abandoned gold and copper tailings impoundment on the eastern slope of the Cascade Mountains in Washington State. The 200- by 46-m impoundment is contained in a narrow valley with steep slopes. A cross section of the impoundment is shown in figure 1. It has an average depth of 6 m and a surface elevation of about 567 m above sea level, and it contains about 33,100 m^3 of material. The phreatic surface, which varies spatially and temporally, is approximately 3 to 4 m below the surface. The valley itself is a surface expression of a northwest-trending, near-vertical, tension-gash fault in midacidic metavolcanic bedrock while

the valley floor is covered with a veneer of remnant gravel. Numerous calcareous and carbonaceous lake beds, some now dry, dot the valley floor. The tailings were deposited on top of the lake sediments and next to a small pond. The upper meter of the silty lake sediments below the tailings are particularly organic rich, but the lateral extent of these sediments is not known. The geology of the valley in which the tailings impoundment was constructed is discussed in more detail by Lambeth (1992).

The gravel aquifer under the tailings is recharged from bedrock sources and local infiltration. The flow direction is from the topographic high at the northwest end of the site toward the topographic low at the southeast end. On the basis of upward gradients between the fractured bedrock and gravel aquifer at locations BKG, M2, and M5 (figure 2), the baseflow in the gravel appears to be locally augmented at certain times of the year by upward groundwater discharge from the fractured bedrock. This ground water probably discharges into the gravel and flows under, around, and possibly into the tailings and the underlying silt. The most likely pathway of water entering the tailings impoundment as meteoric water is down-
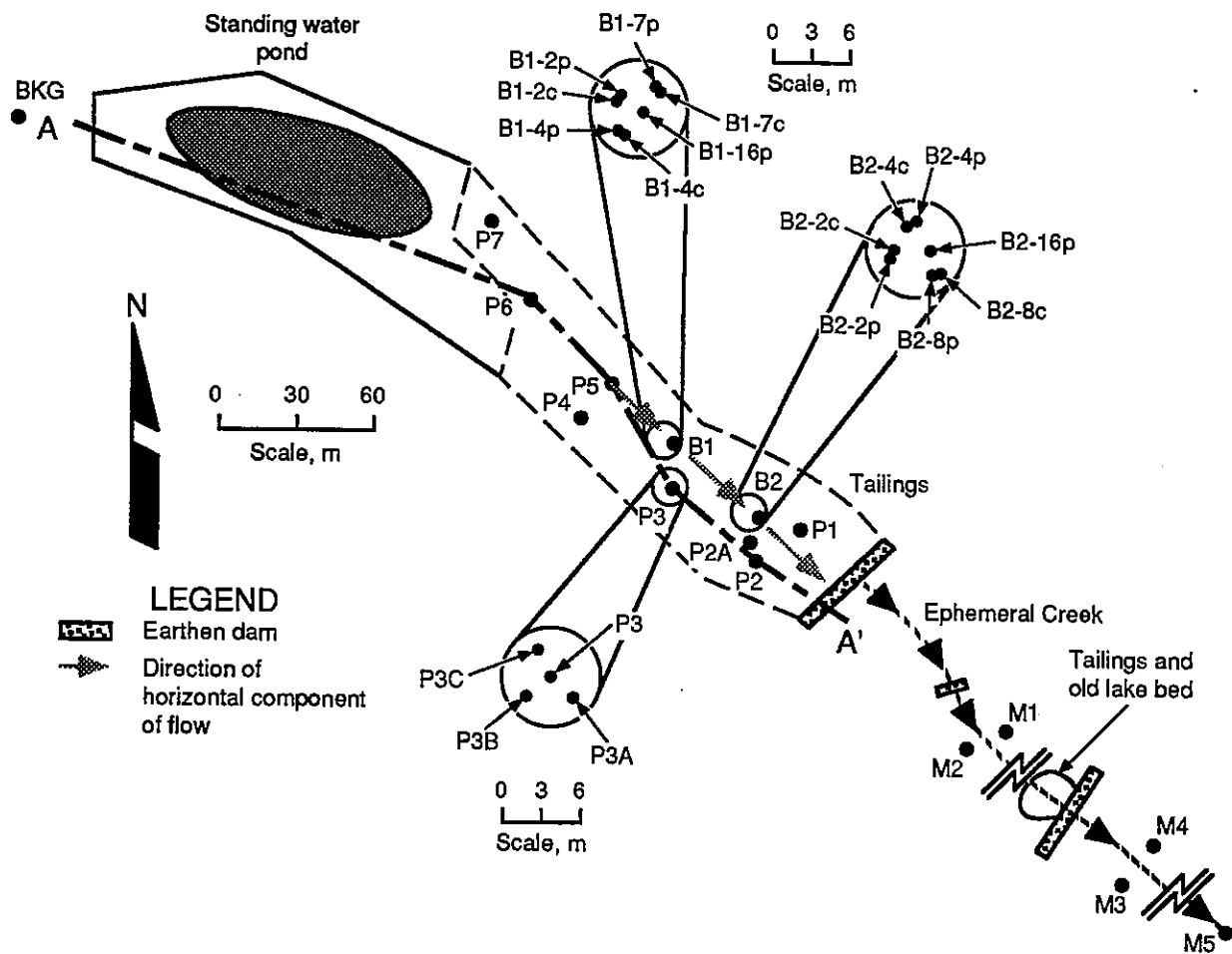
Figure 2. Plan view, research site, and monitoring well locations.

ward through the tailings and the underlying deposits of calcareous and carbonaceous silt and into the gravel aquifer.

There may be some tendency for horizontal flow in the tailings when vertical downward flowlines encounter abrupt boundaries of zones of reduced hydraulic conductivity and are shunted sideways. This horizontal flow may occur along layered heterogeneities in the tailings, such as stratification or hardpan, and also at the contact between the tailings and the underlying organic matter and silts. If substantial horizontal flow does occur at the base of the tailings, it may eventually enter the colluvium at the edges of the impoundment, where the lake sediments stop. The sediment may actually have been removed in the vicinity of the downgradient end of the impoundment when the dam was constructed; if so, downward drainage into the col-

luvium would be enhanced just upgradient of the dam. A substantial evapotranspiration loss may account for some portion of the precipitation mass transfer from the tailings impoundment.

Optical mineralogical examination of tailings from the site indicate that the composition is 95 pct gangue minerals (primarily quartz and plagioclase) and 5 pct sulfide minerals (pyrite > chalcopyrite > sphalerite > > galena). No carbonates from the tailings were observed.

Drilling and Monitoring Well Installation

Forty-one polyvinyl chloride (PVC) and BAT[4] Hydroprobe monitoring wells were in-

---

[4]Reference to specific products does not imply endorsement by the U.S. Bureau of Mines.

220

stalled at the field site in 1987 (see figure 2). These included seven PVC wells (referred to as P wells in this paper) completed in the saturated zone of the tailings, lake sediments, or gravel below the tailings; 14 BAT wells (B wells) completed in the vadose and saturated zones of the tailings; three PVC wells (BKG wells) completed in the gravel or bedrock upgradient of the tailings impoundment; and 17 PVC wells (M wells) completed in the gravel or bedrock downgradient of the impoundment. The BKG and M wells were multiple-completion wells, with two or three PVC piezometers completed at different depths in each hole. The terms BKG-06, M1-02, M4-05, and M5-04 refer to stages of completion in the appropriate multiple-completion well. Wells M1 and M2 were placed on the same pad 15 m apart and 76 m downgradient of the tailings impoundment. Wells M3 and M4 were placed on the same pad 18 m apart and 335 m downgradient, and well M5 was placed on a third pad 550 m downgradient. Well BKG was located approximately 175 m upgradient of the tailings impoundment.

To determine contaminant concentrations below the tailings, three additional wells were drilled in the vicinity of P3 in 1990. These wells, P3A, P3B, and P3C, were drilled to 6.4 m (about 30 cm below the tailings), 5.8 m (base of the tailings), and 7 m (about 90 cm below the tailings), respectively. The 61-cm perforated section of well P3A was placed at the interface between the tailings and the organic-rich layer at the top of the lake sediment, with the upper half of the perforated section in the tailings and the lower half in the organic-rich layer. The perforated section of well P3B was completed in the tailings base and the perforated section of well P3C in the silt below the organic-rich layer. Well P3 (drilled in 1987) was completed at 9.1 m, approximately 3 m in the silt below the tailings and below the organic-rich layer and just above the underlying gravel. Figure 2 shows the research site and the monitoring well locations in plan view.

Field Sampling, Data Collection, and Chemical Analysis

During well construction in 1987 and 1990, samples of tailings material and the sediments below the tailings were obtained using a split-barrel sampler. The samples were used for (1) mineral characterization, (2) determinations of grain size distribution, specific gravity, clay content, and moisture content, (3) sequential digestion of base-metal precipitates, and (4) development of a detailed cross section of the site.

Water samples were collected from all wells approximately every month for 3 years. Water sampling procedures in the PVC wells consisted of purging at least two casing volumes of standing water, filtering the water through an 0.45-micron filter, and acidifying the sample to $pH < 2$. Because of the long recharge time (up to 12 hr) required for the tailings monitoring wells, only one tubing volume was purged for these wells. Details of sampling procedures in the BAT wells are discussed by Williams (1992).

Prior to acidifying, measurements of pH, oxidation-reduction potential (Eh), dissolved oxygen (DO), electrical conductivity (EC), and temperature (T) were taken. When feasible, the electrodes, conductivity cell, and temperature probe were placed in a flow-through chamber. When there was an insufficient amount of the sample to pass through the chamber, measurements were made in a beaker. In addition, duplicate nonacidified samples were collected at all sampling sites, and field alkalinity titrations were made on selected samples. The samples were analyzed for Al, B, Ba, Ca, Cu, Fe, K, Mg, Mn, Na, Ni, Pb, S, Si, and Zn in the laboratory using an inductively coupled plasma emission spectrometer (ICP). The unpreserved samples were analyzed with an ion chromatograph for Cl^{1-} and SO_4^{2-}.

Other important data collected included depth-to-water, hydraulic conductivity using the BAT system, and tailings moisture content and bulk density at various depths and locations us-

Table 1. Arithmetic means of analyses and chemical parameters (concentrations in mg/L).

	BKG-06	TAILS	M1-02	M4-05	M5-04
ph	7.1	4.2	5.9	6.8	7.1
EC (μS/cm) . .	490	9,200	1,000	2,400	1,800
Eh (mV)	400	440	410	410	360
HCO_3^{1-}	340	0	0	480	440
Al	0.21	700	0.84	0.38	0.34
B	0.18	28	0.63	0.32	0.29
Ba	0.03	0.03	0.04	0.04	0.06
Ca	140	470	480	610	390
Cd	<0.01	4.9	<0.01	<0.01	<0.01
Cl	5	200		10	10
Cu	0.05	79	0.24	0.10	0.08
Fe	0.77	10,000	260	0.57	0.64
K	2.3	47	14	8.7	4.3
Mg	29	1,800	280	210	120
Mn	0.03	130	31	1.9	0.42
Na	20	30	23	30	53
Ni	<0.05	2.3	0.21	<0.05	<0.05
Pb	0.06	3.7	0.11	0.09	0.07
S	92	11,000	920	730	390
SO_4^{2-}	230	49,000	2,500	2,200	1,000
Si	14	31	23	19	15
Zn	0.11	1,200	56	0.39	0.16

ing a downhole neutron/gamma density-moisture gauge. Groundwater flow velocities and directions at M1 and M5 in the shallow alluvium were determined by borehole-to-surface DC resistivity techniques (Sill and Sjostrom, 1990).

Results

Several factors have an impact or potential impact on contaminant migration and attenuation at the study site. These factors include physical, hydrologic, and hydrogeochemical properties of the waste impoundment and the environment around the waste impoundment.

Water Quality

Because of the large amount of water quality data collected at the study site, average concentrations are reported here only from 14 key wells of the 45 wells sampled. Mean concentrations from all wells can be found in Lambeth (1992) and Williams (1992). Examination of the data illustrates that the downgradient plume is best represented by samples from the shallowest piezometers in wells M1, M4, and M5. Data from the shallowest piezometer in well BKG were used to represent groundwater quality upgradient of the impoundment; mean concentrations were determined for the impoundment pore water (tailings) with data from P4, P5, P6, and two BAT devices in the saturated zone, B1-16p and B2-16p (tables 1 and 2). Downgradient reduction of soluble Fe concentrations, as well as other trace metals such as Cu, Pb, and Zn, is extremely rapid upon leaving the tailings. Concentrations of all metals except Ca, Mg, Mn, Na, and S were less than twice background levels at well M5, 550 m downgradient from the impoundment. Also at well M5, pH was the same as background levels of 7.0 (Lambeth, 1992).

Table 2. Mean[1] constituent concentrations in well clusters B1 and B2[2], mg/L.

Constituent	Location					
	B1-4p	B1-7p	B1-16p	B2-4p	B2-8p	B2-16p
pH	3.76	3.73	3.49	3.16	3.74	3.89
Depth,[3] m	1.2	2.1	4.8	1.2	2.4	4.8
Element:						
Al	55	582	2,749	552	501	147
Ca	96	466	531	428	451	458
Cu	15	113	16	137	102	50
Fe	75	811	12,864	2,013	1,194	763
K	12	4	59	2	6	4
Mg	93	372	2,429	329	416	155
Mn	2	9	159	8	17	2,917
Na	6	36	38	17	29	17
Pb	0.2	0.4	5	0.7	0.7	2
S	366	2,303	15,614	3,013	2,531	1,317
Si	70	49	41	100	34	32
Zn	7	46	1,539	140	178	78

[1]Means were calculated on analyses of 14 to 16 different water samples collected over 2 years.

[2] Well cluster B2 is approximately 46 m southeast of well cluster B1.

[3] Depths from ground level to center of porous sampling tip.

Examination of mean water quality data from the two clusters of BAT devices (table 2) (Williams, 1992) illustrates that the saturated pore water in the tailings generally had higher concentrations of metals than the pore water in the vadose zone, even though the vadose water generally had lower pH and higher oxidation potential. This indicates that highly soluble constituents of the vadose zone have already been leached. Mean concentrations of contaminants in wells P3A, P3B, and P3C are shown in table 3. Results indicate that concentrations in solution decreased rapidly with depth below the tailings.

Physical Properties

The vertical and horizontal seepage rates of water in the tailings are probably influenced by the large reduction in grain size with depth. Grain size distributions in composite samples at depths between 1.5 and 2.1 m and between 4.9 and 5.8 m near well P3 are shown in figure 3. At well P3 and at least two other locations, a layer of tailings containing silt-sized particles 60 to 90 pct finer than 0.02 mm lies at the base of the impoundment. The higher percentage of fines at increased depth may exist for many reasons. (1) A greater portion of fines in the vadose zone may already have dissolved, (2) some portion of the fines in the saturated zone may be precipitated oxidation products from constituents leached out of the overlying material, (3) some of the fines in the vadose zone may have been cemented into larger, agglomerated particles, or (4) some portion of the fines resulting from weathering in the vadose zone may have been transported downward with time.

The change in grain-size distribution with depth may be correlated to the fact that water samples from the saturated zone have higher concentrations of many key elements than do samples from the vadose zone. Because finer materials have more surface area available for chemical interaction which leads to more rapid dissolution, highly soluble fines in the vadose zone have probably already been dissolved.

Table 3. Mean constituent concentrations below tailings.

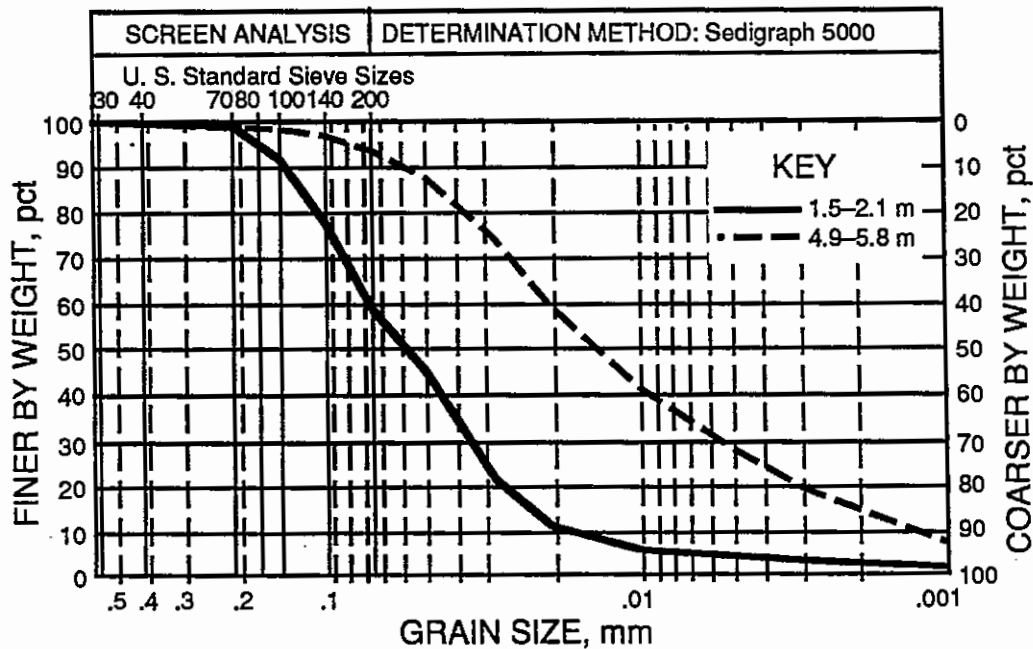| Constituent	P3B, base of tailings	P3A, 30 cm below tailings	P3C, 90 cm below tailings	P3, 305 cm below tailings
pH	6.1	6.4	6.6	6.9
Conductivity, μS/cm . . .	3,448	2,456	1,630	1,788
Eh, mV	230	215	181	220
HCO_3, mg/L	473	674	574	553
Element, mg/L:				
Al	1.25	0.57	0.33	0.30
B	2.6	0.69	0.56	0.30
Ba	0.04	0.07	0.08	0.09
Ca	536	508	391	363
Cu	0.58	0.17	0.09	0.07
Fe	968	233	197	9.2
K	54.3	22.8	12.4	1.9
Mg	610	361	145	127
Mn	74	22	6.5	0.08
Na	65	38	25	38
Pb	0.21	0.11	0.1	0.06
S	1,887	893	504	354
Si	21	16	18	25
Zn	4.5	2.8	0.93	0.35

Figure 3. Grain-size distribution of samples from vadose zone (solid line) and saturated zone (dotted line) from well P3A.

It is important to note that the increase in the percentage of fines with depth in the impoundment will reduce hydraulic conductivity with depth.

Physical (and chemical) heterogeneities are not uncommon in milled tailings impoundments, and this study site is no exception. Spatial variability of properties in tailings piles can result

224

from differences in ore mineralogy, short-term changes in milling processes, depositional history, or weathering after deposition. The tailings at the study site are layered, and layers differ on the basis of color, texture, grain size, density, and moisture content. The influence of these physical heterogeneities on water chemistry and water movement may vary depending on locality.

The moisture content and density profile at well B2-4c (figure 4) shows an isolated layer of high moisture and low density in the vadose zone about 46 cm below the surface. A tailings sample was collected from the surface to a depth of 61 cm through this layer near well B2-4c and examined. In the middle of the sample was a hardpan layer. The hardpan sample did not soften or decompose when it was exposed to water or concentrated acid. The tailings above the hardpan appeared to be more oxidized, much lower in moisture content, and coarser in grain size than the tailings below the hardpan.

The grain-size distributions of samples above and below the hardpan are shown in figure 5. A
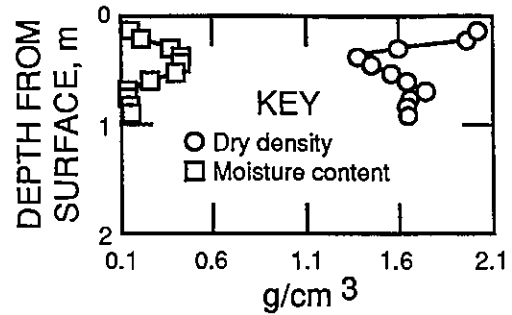
Figure 4. Moisture content and density profile in unsaturated tailings at well B2-4c.

dramatic reduction in grain size between the top and bottom of sample B2 can be seen. The explanation of this large difference, although not clear, possibly relates to the chemical and physical weathering of particles, or perhaps the cementation of particles above the hardpan but not below.

The hardpan in the B2 sample divides coarse and fine tailings and restricts the downward flow of pore water and atmospheric oxygen. This has two effects on contaminant migration and attenuation. First, because oxidation is re-
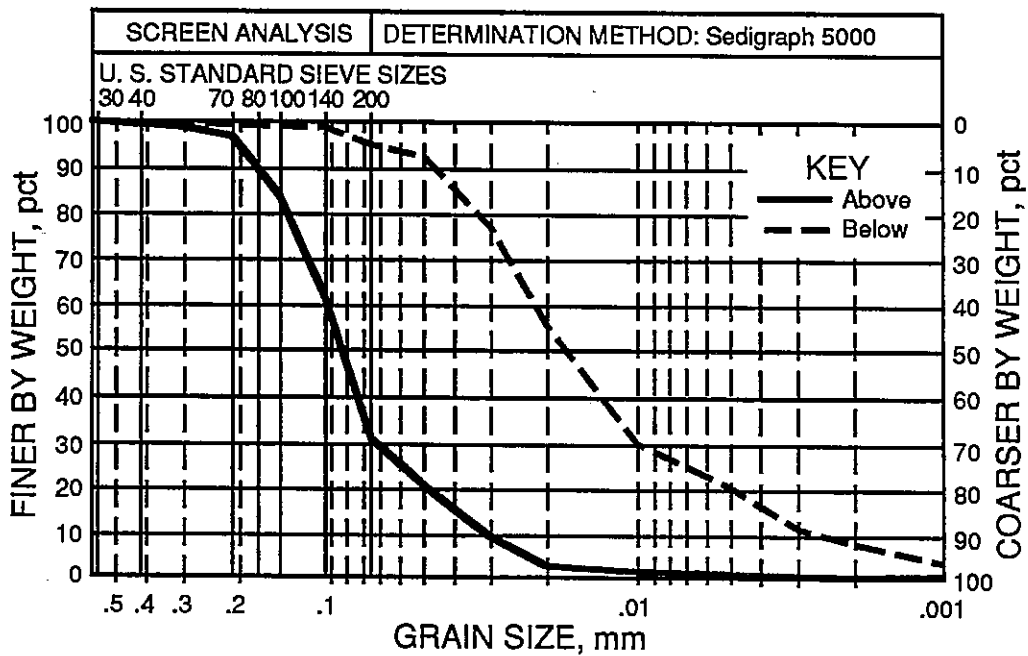
Figure 5. Grain-size distribution in samples from above (solid line) and below (dotted line) hardpan. The samples were collected in a zone extending from the surface to a depth of 76 cm near well B2.

225

quired in the acid generation process, acid generation below the hardpan is slowed. Second, the hardpan appears to impact pore water quality. The data (table 2) indicate that concentrations of most metals in solution decrease with depth at the B2 location but increase at the B1 location. This difference may be related to the hardpan within the B2 cluster. By restricting flow through the hardpan and the finer material below, the H^+ ion may be given enough residence time to consume the neutralizing agents of silicate and aluminosilicate mineral dissolution, resulting in more sulfide oxidation products in solution at the 1.2-m level. At B1, where there is no hardpan, the downward progression of H^+ lags behind the downward progression of the sulfide oxidation products, resulting in higher metal concentrations and lower pH with depth.

Similar findings were reported at the Heath Steele Mine's tailings dump in New Brunswick (Boorman and Watson, 1976). The Canadian researchers describe the hardpan as being 5 to 10 cm thick, lying 25 to 50 cm below the surface between the oxidation zone and the reduction zone, and consisting of tailings cemented with iron hydroxides, oxides, and gypsum. In addition, the hardpan contained high levels of copper and zinc that precipitated as a result of chemical reactions. In 1985, the pore water chemistry at the Heath Steele tailings dump was found to be about the same as it was in 1976. The consistency of the geochemistry over the 9-year period was attributed to the effect of the hardpan (Blowes et al., 1987).

Solid samples collected during initial drilling clearly indicate the tailings were deposited in a shallow, swampy lake basin. Below the tailings is an organic-rich silt layer 30 to 60 cm thick containing abundant snail shells. Below this layer is a formation of silts 3 to 4.5 m thick. An energy-dispersive scanning spectrum of this material showed abundant Si and detectable amounts of Al, K, Ca, and Fe. Figure 6 illustrates that at a depth of 5.8 m the silt zone has a lower density than the tailings and contains 1.7 times more water by weight per unit volume than the tailings. The average water content and
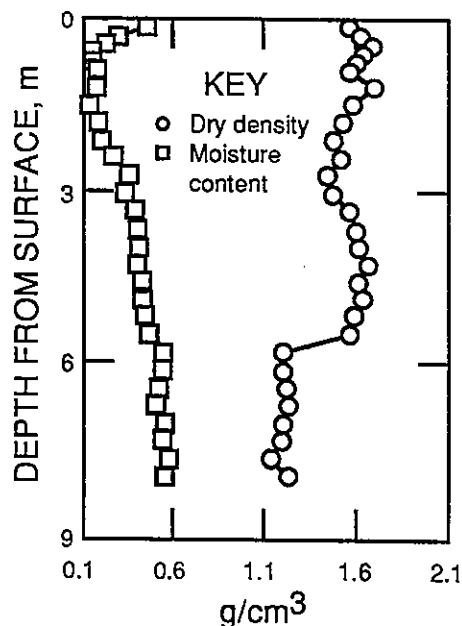

Figure 6. Moisture content and density profile in tailings and silts below tailings near well P3. Changes between the two units are noticeable at 5.8 m.

bulk density of the silt below the tailings at P3 (measured in June 1989) were 46.9 pct by weight and 1.17 g/cm³, respectively. By comparison, the average water content and bulk density in the saturated tailings at P3 were 27 pct and 1.60 g/cm³, respectively. Using the average bulk densities measured in June 1989 and the average specific gravity of solids in each zone (determined by specific gravity tests on samples collected at the study site), the porosity for the saturated tailings was 42.8 pct and for the saturated silt 54.4 pct. These measurements were consistent with the presence of the organic material underlain by lacustrine silt, as identified during drilling.

Hydrologic Properties

Based on three-point solutions of average potentiometric elevations among wells P4, P5, and P6, and among wells P4, P5, and P1, the direction of the horizontal component of flow from well P5 was determined (shown by an arrow on figure 2). The potentiometric surface

in the direction of flow dips about 0.78 m between P6 and P1, a distance of about 140 m, resulting in a relatively flat horizontal hydraulic gradient of 5.6×10^{-3}. This was compared to an even flatter horizontal gradient of 6.0×10^{-4} from well P5 to well P4. Downgradient horizontal hydraulic gradients were 3.9×10^{-2} and 2.2×10^{-2} between the shallowest piezometers of wells M2 and M4 and between the shallowest piezometers of wells M4 and M5, respectively. Spacing between wells in the saturated tailings were inadequate for determining the vertical component of the hydraulic gradient. In situ measurements determined with the BAT system indicated an average hydraulic conductivity in the saturated tailings of 2×10^{-5} cm/s.

Fifty years after the tailings were deposited onto the silts, concentrations of every element determined (except Ba) were lower in the pore water of the silts 30 to 90 cm below the tailings than in the pore water at the base of the tailings (table 3) and much lower than in the pore water in the core of the saturated tailings (Lambeth, 1992). This could indicate that water with very low concentrations of measured constituents is flushing the porous silts and perhaps the base of the tailings. At the P3 cluster (wells P3, P3A, P3B, and P3C), the vertical component of gradient indicated a weak upward flow in the lacustrine sediments during the spring, a time of high discharge.

Another explanation for low metal concentrations in the silts below the tailings is that tailings pore water may not be seeping into the silts to any significant degree, but may be diverted laterally as horizontal flow induced by an abrupt reduction in hydraulic conductivity at the contact between the tailings and the underlying organic layer and silt. If substantial horizontal flow does occur at the base of the tailings, then pore water from the tailings may eventually enter the gravels at the edges of the impoundment, by-passing the organic material and silts. The degree of mixing between tailings pore water and colluvium water is unknown. However, the geochemical modeling discussed below includes mixing ratios.

A third explanation for the low concentrations in the silts is that the neutralizing capacity of the calcareous silt could be inducing precipitation, which would decrease metal concentrations in the silt pore water.

Other hydrologic properties that may affect downgradient contaminant transport at the study site are advection and dispersion. Based on the difference in estimated horizontal groundwater flow velocities (2.7×10^{-4} m/day in the saturated tailings and 0.6 m/day in the downgradient aquifer) (Stewart et al., 1990; Sill and Sjostrom, 1990), the transport of contaminants by flowing ground water (advection) is much greater in the downgradient aquifer than in the tailings. The advective velocity of nonreactive or nonretarded constituents downgradient from the impoundment is equal to the average horizontal downgradient groundwater velocity. Because of the confined nature of the shallow aquifer at this site, dispersion is limited and probably occurs in the longitudinal rather than in the horizontal or vertical plane of the flow path.

Hydrogeochemical Properties

Based on the previously described hydrology of the site and commonly accepted views concerning acid production and contaminant transport, the following sequence of events is thought to occur.

1. Meteoric water infiltrates through the vadose zone of the tailings impoundment, where the oxidation of sulfide minerals produces dissolved metal and sulfuric acid, which in turn attack silicate and other minerals. Evaporation removes some fraction of water from the vadose zone, particularly during June, July, and August, and may leave behind efflorescent salts.

2. The remaining recharge continues generally downward into the saturated zone where it may mix with upgradient ground water flowing into the tailings.

3. The pore water leaves the impoundment. Some of this water mixes directly with the underlying ground water, but a portion of it passes through the calcareous, carbonaceous lacustrine sediment beneath the tailings, where it is partially neutralized prior to entering the groundwater stream. Chemical precipitation probably begins in the mixing zone.

4. As the resultant plume moves within the gravel downgradient of the dam, it continues to mix with surface infiltration water and perhaps ground water discharging from underlying fractures. Rapid downgradient attenuation occurs as a result of mixing and a variety of chemical reactions that induce precipitation. Oxidation may be a dominant control mechanism.

Coprecipitation, ion exchange, and sorption are also potential major attenuation factors. However, the aquifer is composed of gravel with little silt or clay; most of the particles are metavolcanic materials. There is little in this material to suggest significant exchange or sorption of the magnitude necessary to account for the degree of attenuation found at this location. Therefore, precipitation and coprecipitation are probably the major controlling chemical mechanisms downgradient.

Geochemical modeling. To assess the roles of chemical dissolution, mixing, and precipitation as controlling mechanisms at this site, a two-step process using two separate computer models, WATEQ4F (Ball and Nordstrom, 1991) and BALANCE (Parkhurst et al., 1982), were used. Both codes are available from the U.S. Geological Survey and are widely used. WATEQ4F is an ion speciation model that utilizes analytical data and field parameter information to calculate saturation indices of a wide variety of minerals. The model will predict whether, under field conditions, a given mineral has a tendency to dissolve or precipitate or whether it is in equilibrium, but it does not consider reaction kinetics. BALANCE performs mass balance computations of dissolved constituents between two points on a flow path given a suite of mineral phases. These phases are allowed to either dissolve, precipitate, or both dissolve and precipitate. The user establishes these constraints on the basis of his or her knowledge of the mineralogy at the site in conjunction with saturation indices determined by WATEQ4F. For example, minerals such as albite and anorthite can dissolve but could not precipitate at the temperatures and low pressures of a shallow aquifer even though the WATEQ4F simulation indicates extreme oversaturation for these minerals.

WATEQ4F and BALANCE are interpretive tools capable of predicting only the likelihood of mineral dissolution or precipitation. Ion exchange reactions can be simulated within BALANCE, if specifically defined by the user, but adsorption cannot be directly simulated. Therefore, the code will attribute to precipitation a concentration change that may be caused by adsorption. BALANCE also contains an electron-accounting function for redox reactions; oxygen was used as the primary oxidant. Carbon dioxide concentrations were calculated from alkalinity measurements. Mixing of waters can also be simulated by BALANCE; this capability was extensively used during this project. To use BALANCE defensibly, the user must determine that the two endpoints of the mass balance simulation are on a flowpath. The flowpath segments analyzed below are considered to be probable at this site. The groundwater flow in the tailings and in the colluvial aquifer are assumed to be equilibrated and steady-state, because no cyclical trends in water quality have been observed in over 2 years of intensive sampling. Longer term trends are, of course, possible.

The simulation procedure is as follows.

1. The sample analyses from the two endpoint wells for each segment along the flowpath were processed through WATEQ4F.

Table 4. Ion balances, ionic strengths, and saturation indices of WATEQ4F simulations.
(Parentheses indicate the mineral will not form a stable phase.)
(Values for minerals are saturation indices.)

	BKG-06	P4	P5	P6	B1-16p	B2-16p	M1-02	M4-05	M5-04
Ion balance (%) . .	-3.2	-6.2 to 7.7	-4.2 to 2.6	-3.3	6.8	-6.1 to 7.8	2.2	11.0	-2.4
Ionic strength . .	0.015	0.51 to 0.55	0.44 to 0.5	1.3	0.8	0.091 to 0.097	0.061	0.06	0.043
Allophane	(1.7)	-0.4 to 0.56	-0.8 to -0.5	-1.1	-0.6	-1.0 to -0.82	0.48	(1.7)	(2.0)
Alunite	(3.5)	6.0 to 11.0	3.5 to 5.4	1.5	4.3	-1.5 to 2.0	(5.8)	(10.0)	(7.0)
Anglesite	-3.5	-0.4 to 0.26	0.063 to 0.3	0.6	0.42	-0.081 to -0.066	-1.6	-1.7	-2.2
Barite	0.95	0.41 to 1.3	0.67 to 2.7	0.58	0.47	0.25 to 0.27	0.71	NA	1.5
Basaluminite . . .	(8.4)	1.0 to 9.5	-1.0 to 1.7	-4.4	-2.5	-9.0 to -2.7	(6.6)	(6.6)	(12.0)
Cerrusite	-0.57	NA	NA	NA	NA	NA	NA	-0.25	-0.000
Ferrihydrite . . .	3.5	-0.56 to 1.2	-1.4 to 1.0	0.36	-0.11	-1.3 to -1.6	5.3	2.0	3.3
Gibbsite	3.1	-0.52 to (2.0)	-1.4 to -0.56	-1.9	-1.9	-3.2 to -1.7	1.8	3.7	3.7
Gypsum	-1.0	0.07 to 0.27	0.1 to 0.25	0.5	0.32	0.028 to 0.045	-0.95	0.009	-0.21
Jarosite-H	-7.2	-5.6 to -1.4	-4.9 to 1.1	-2.4	0.32	-6.3 to -4.4	(4.8)	-6.5	-6.1
Jarosite-K	0.81	0.8 to 5.0	0.21 to 5.5	4.2	5.7	-1.8 to -0.6	(12.0)	0.9	(1.8)
Jarosite-Na	-2.1	-3.1 to 0.9	1.8 to 3.5	-0.43	1.3	-5.0 to -3.7	(8.5)	-2.3	-1.1
Jurbanite	-2.3	1.2 to 2.2	1.8 to 2.0	-0.11	1.9	0.45 to 0.99	-0.2	0.96	-0.78
Kaolinite	(8.8)	2.8 to 7.4	0.92 to 2.1	-0.35	-0.058	-3.2 to -0.08	(6.4)	(10.0)	(9.8)
Magnesite	-0.9	NA	NA	NA	NA	NA	NA	-1.2	-0.59
Melanterite	-9.4	-0.79 to -0.74	-0.91 to -0.81	0.003	-0.51	-2.1	-5.9	-5.5	-6.2
Ca-montmorillonite.	8.6	(1.4) to (7.0)	-0.94 to 0.37	-2.3	-2.1	-6.2 to -2.3	5.6	10.0	9.7
Montmorillonite . .	7.1	0.19 to (5.3)	-2.3 to -0.89	(1.9)	-2.6	-6.8 to -4.0	4.9	7.1	7.7
Rhodochrosite . . .	-2.2	NA	NA	NA	NA	NA	NA	-1.7	-0.93
SiO$_2$(a)	-0.47	-0.11 to 0.18	-0.48 to 0.09	-0.56	0.14	-0.15 to -0.11	-0.37	-0.42	-0.54
Siderite	-3.9	NA	NA	NA	NA	NA	NA	-1.6	-1.4
Adularia	(2.7)	-1.0 to (2.5)	-5.8 to -2.4	-2.4	-3.0	-6.7 to -4.3	(1.1)	(3.0)	(3.1)
Albite	(1.2)	-3.3 to -0.34	-5.7 to -0.48	-5.7	-6.1	-8.4 to -6.3	-1.2	(1.1)	(1.5)
Anorthite	(1.0)	-11.0 to -4.6	-14.0 to -13.0	-13.0	-15.0	-19.0 to -15.0	-3.8	0.75	(1.9)
Chlorite	-5.8	-33.0 to -20.0	-43.0 to -40.0	-32.0	-44.0	-55.0 to -47.0	-17.0	-10.0	(3.3)
Quartz	0.91	0.91 to (1.5)	0.91 to (1.5)	(1.3)	(1.5)	(1.2) to (1.3)	1.0	0.96	0.85
Calcite	0.26	NA	NA	NA	NA	NA	NA	-0.24	0.39

2. A list of all oversaturated or equilibrated secondary minerals and undersaturated or equilibrated ion source minerals was compiled for each well.

3. Stability diagrams for each secondary mineral were then examined to determine if it were probable that the mineral would actually form under the specific field conditions. The list of potential precipitates between each well was thus reduced.

4. The mean analysis for each well was then processed through BALANCE utilizing the source and sink phases determined above. The program determines what combinations of phases satisfy mass balance changes along the flow segment.

5. The successful combinations determined by BALANCE were examined to determine which were most logical.

From the tabulation of logical BALANCE solutions the mechanisms of attenuation could then be inferred.

The segments used during this investigation were Rainwater to Tailings Pore Water, Tailings Pore Water to M1-02, M1-02 to M4-05, and M4-05 to M5-04. The saturation indices of the selected phases for each of the above wells are shown in table 4. These values were selected only from the WATEQ4F simulations that achieved a calculated difference in the cation\anion balance of approximately 10 pct or less. For some wells (P4, P5, and B2), this included a range of sample values (table 4).

On the bases of the mineralogy of the tailings and the common and extensive presence of propyllitized andesite, the most probable source minerals for dissolved ions are potassium feldspar, albite, anorthite, chlorite, and quartz. The sulfide minerals in the tailings that act as metal and sulfate ion sources are chalcopyrite (Cu, Fe, S), galena (Pb, S), pyrite (Fe, S), and sphalerite (Zn, S). In addition, because of the abundance of shells, the lake sediments are a source of cal-

cite or aragonite. The list of potential precipitates includes allophane, alunite, anglesite, barite, basaluminite, cerrusite, ferrihydrite, gibbsite, gypsum, jarosite-H, jarosite-K, jarosite-Na, jurbanite, kaolinite, magnesite, melanterite, Ca-montmorillonite, montmorillonite, rhodochrosite, amorphous SiO_2, siderite, and calcite. The thermodynamic constants for the potential precipitates are reasonable except for allophane and the montmorillonites. There is much controversy concerning the ability of montmorillonites to precipitate directly from solution under any circumstances. Some of these phases, most notably magnesite, require extreme supersaturation in order for precipitation to begin.

The results of the BALANCE simulations for the selected segments are summarized as follows.

Segment 1—Rainwater to Tailings Pore Water

The most successful BALANCE simulation for explaining oxidation in the impoundment was achieved by using water having the composition of east Seattle rainwater (INIT 1). This water was allowed to react with the tailings minerals to form acidic pore water, and the mixing function of the model was activated using background water with the mean composition of BKG-06 (INIT 2). No successful solutions resulted if background water was mixed with the rain water. Albite, anorthite, chlorite, potassium feldspar, oxygen, chalcopyrite, galena, pyrite, and sphalerite were used as sources; allophane, alunite, anglesite, basaluminite, ferrihydrite, gypsum, jarosite, kaolinite, melanterite, and amorphous silica were used as sink phases.

```
                BALANCE Results:

1,352,078 MODELS WERE TESTED.
       20 MODELS WERE FOUND WHICH SATISFIED
          THE CONSTRAINTS.
        4 MODELS WERE FOUND WHICH SATISFIED
          THE CONSTRAINTS AND DID NOT REQUIRE
          EXCESSIVE DISSOLUTION OR
          PRECIPITATION.

Preferred solutions ( PHASE; - = PHASE can only
precipitate, + = PHASE can only dissolve; F = all
solutions  must  include  PHASE;  mmol/L,  -  =
precipitation, + = dissolution; mix ratio INIT
1:INIT 2):
```

Phase			mmol/L	Mix ratio
INIT 1	+	F	1.0000	1:0
INIT 2	+	F	0.0000	
ALBITE	+		1.2900	
ANORTH	+		50.0270	
CHLORITE	+		9.7998	
GYPSUM	-		-38.0290	
K-FELDSP	+		1.1980	
KAOLINIT	-		-48.0708	
O2 GAS			666.0360	
PYRITE	+		178.8000	
SiO2			-39.6778	
CHALCOPY	+		1.2000	
GALENA	+		0.0180	
SPHALERT	+		18.0000	
INIT 1	+	F	1.0000	1:0
INIT 2	+	F	0.0000	
ALBITE	+		1.2900	
ANORTH	+		34.0034	
CHLORITE	+		9.7998	
GYPSUM	-		-22.0054	
K-FELDSP	+		1.1980	
O2 GAS			666.0360	
PYRITE	+		178.8000	
SiO2			-103.7722	
CHALCOPY	+		1.2000	
GALENA	+		0.0180	
SPHALERT	+		18.0000	
BASALUNT	-		-16.0236	

All solutions utilized albite, anorthite, chalcopyrite, galena, gypsum, potassium feldspar, oxygen, pyrite, and amorphous silica precipitate. No solutions included alunite, anglesite, carbon dioxide, ferrihydrite, jarosite, or melanterite. The most logical solutions in view of precipitate stabilities were achieved when excess Al (resulting from aluminosilicate dissolution) was precipitated as kaolinite or basaluminite.

Segment 2— Tailings Pore Water to M1-02

Albite, calcite, chlorite, potassium feldspar, and oxygen were used as source phases; allophane, alunite, basaluminite, carbon dioxide, ferrihydrite, gibbsite, gypsum, hydro-potassium-natro jarosites, jurbanite, kaolinite, calcium-potassium-sodium-magnesium montmorillonites, melanterite, and amorphous silica were utilized as sink phases. Tailings pore water (INIT 1) was allowed to mix with background water (INIT 2) from BKG-06. Because the tailings pore water was flowing from an acidic to a more neutral environment, both acidic and nonacidic phase precipitates were incorporated. Because it would be unrealistic to allow the dissolution of

large amounts of silicate minerals in transition from acid to neutral conditions, the amount of silicate minerals in successful solutions · was arbitrarily limited to 1 mmol/L.

BALANCE Results:

817,190 MODELS WERE TESTED.
    564 MODELS WERE FOUND WHICH SATISFIED THE CONSTRAINTS.
    140 MODELS WERE FOUND WHICH SATISFIED THE CONSTRAINTS AND REQUIRED DISSOLUTION OF LESS THAN 1 MMOL/L OF ALBITE AND K-FELDSPAR.
    129 MODELS RESULTED FROM THE MOST REALSTIC MIX RATIO OF 1:5.74. OF THESE 79 INCLUDED MELANTERITE WHILE 50 DID NOT.

Preferred solutions (PHASE; - = PHASE can only precipitate, + = PHASE can only dissolve; F = all solutions must include PHASE; mmol/L, - = precipitation, + = dissolution; mix ratio INIT 1:INIT 2):

Phase			mmol/L	Mix ratio
-Without Melanterite-				
INIT 1	+	F	0.1484	1:5.74
INIT 2	+	F	0.8516	
CO2 GAS	-		-35.9176	
GIBBSITE	-		-4.0309	
GYPSUM	-		-23.9093	
K-FELDSP	+		0.1317	
O2 GAS	+		4.6172	
SiO2	-		-0.3628	
FERRIHYD	-		-22.0152	
CALCITE	+		31.1484	
ALBITE	+		0.0662	
-With Melanterite-				
INIT 1	+	F	0.1484	1:5.74
INIT 2	+	F	0.8516	
CO2 GAS	-		-17.4488	
GIBBSITE	-		-4.0309	
GYPSUM	-		-5.4406	
K-FELDSP	+		0.1317	
SiO2	-		-0.3628	
FERRIHYD	-		-3.5465	
MELANTRT	-		-18.4687	
CALCITE	+		12.6796	
ALBITE	+		0.0662	

Chlorite was the only sink phase not utilized in any successful solution. The most interesting thing to note here is that two distinct mechanistic pathways were indicated. In the first pathway, oxidation combined with neutralization was the controlling mechanism, and excess Fe and Al were precipitated as ferrihydrite and gibbsite. Phases common to all solutions of this pathway were albite, calcite, carbon dioxide, gypsum, potassium feldspar, and oxygen. The mix ratio was 1 part tailings pore water to 5.74 parts

231

background water. The second pathway required the precipitation of large quantities of melanterite and lesser amounts of ferrihydrite to account for the loss of Fe. Melanterite normally precipitates as an efflorescent salt; however, it was equilibrated in most samples from the impoundment. This would indicate that melanterite was poised and could precipitate, especially during the hot, dry summer months when evapotranspiration is at its peak. Although calcite from the lacustrine sediments was consumed in lesser quantities in the second pathway than in the first, the controlling mechanism appeared to be predominantly neutralization because very little oxygen was consumed in this second pathway. The dominant Al control in the second pathway was also precipitation of gibbsite. Phases common to all solutions of this pathway were albite, calcite, carbon dioxide, potassium feldspar, and melanterite. Oxygen was not a common phase, but it was consumed in minor amounts in a few solutions. The mix ratio was again 1 part tailings pore water to 5.74 parts background water. No secondary trace metal precipitates were oversaturated along this segment; however, anglesite was equilibrated within the impoundment.

During a separate simulation, when anorthite was used as a Ca source, no solutions were obtained.

Segment 3— M1-02 to M4-05

In this segment albite, calcite, chlorite, potassium feldspar and oxygen were used as source phases; ferrihydrite, gibbsite, gypsum, magnesite, calcium-potassium-magnesium-sodium montmorillonite, and amorphous silica were used as sink phases; carbon dioxide was permitted to be either. Five successful solutions were obtained from 5,005 models tested by the code. A mix of 1 part background water (BKG-06) and 3.35 parts water with the composition of M1-2 was required. The authors would have preferred to use ground water emanating from fractured bedrock during mixing simulations. However, significant ion exchange of Ca and Mg for Na from the bentonite well sealant was identified in the deep piezometers (Lambeth,

1992). Therefore, the use of water with the composition of BKG-06 was the only alternative source.

```
          BALANCE Results:

 5,005 MODELS WERE TESTED.
    14 MODELS WERE FOUND WHICH SATISFIED THE
       CONSTRAINTS.
     5 MODELS WERE FOUND WHICH SATISFIED THE
       CONSTRAINTS AND REQUIRED DISSOLUTION OF
       LESS THAN 1 MMOL/L OF ALBITE AND
       K-FELDSPAR.
```

Preferred solution (PHASE; - = PHASE can only precipitate, + = PHASE can only dissolve; F = all solutions must include PHASE; mmol/L, - = precipitation, + = dissolution; mix ratio INIT 1:INIT 2):

Phase		mmol/L	Mix ratio
INIT 1	+ F	0.7701	3.35:1
INIT 2	+ F	0.2299	
ALBITE	+	0.3299	
CALCITE	+	4.9540	
CO2 GAS		2.5759	
GIBBSITE	-	-0.4933	
K-FELDSP	+	0.1787	
MAGNESIT	-	-0.9172	
O2 GAS	+	1.6429	
SiO2	-	-1.6022	
FERRIHYD	-	-3.6128	

Only one model was a preferred solution; it utilized gibbsite, ferrihydrite, and magnesite to account for attenuation of Al, Fe, and Mg beyond that achieved by mixing. Magnesite precipitation requires extreme supersaturation, and its inclusion was speculative. Chlorite and gypsum were not contained in any of the successful solutions, but oxygen was contained in every solution. This may indicate that oxidation was a dominant chemical attenuation mechanism. Other phases common to all solutions were albite, calcite, carbon dioxide, ferrihydrite, potassium feldspar, magnesite, and amorphous silica. Using anorthite as a Ca source did not provide realistic results, but there did appear to be an old lake bed just upgradient from M4 that could provide Ca and bicarbonate ions from reactions of shell dissolution. There were no secondary trace element minerals predicted by WATEQ4F to be oversaturated.

Segment 4— M4-05 to M5-04

In this segment, albite, anorthite, chlorite, and potassium feldspar were used as source

phases; calcite, ferrihydrite, gibbsite, gypsum, magnesite, calcium-potassium-magnesium-sodium montmorillonite, rhodochrosite, and amorphous silica were input as sink phases; carbon dioxide was permitted to be either. There is no plausible source for calcite as a source phase; anorthite was used instead. No solutions were obtained when electron accounting was considered; therefore, oxygen could not be used as a source phase. No successful solutions were obtained that required dissolution of less than 1 mmol/L of silicate minerals, and the requirement was raised to 10 mmol/L for maximum-minimum silicate dissolution.

```
            BALANCE Results:

11,440 MODELS WERE TESTED.
    57 MODELS WERE FOUND WHICH SATISFIED THE
       CONSTRAINTS.
    33 MODELS WERE FOUND WHICH SATISFIED THE
       CONSTRAINTS AND REQUIRED DISSOLUTION OF
       LESS THAN 10 MMOL/L OF ALBITE AND
       K-FELDSPAR.
```

Preferred solution (PHASE; - = PHASE can only precipitate, + = PHASE can only dissolve; F = all solutions must include PHASE; mmol/L, - = precipitation, + = dissolution; mix ratio INIT 1:INIT 2):

Phase		mmol/L	Mix ratio
INIT 1	+ F	0.4527	1:1.21
INIT 2	+ F	0.5473	
ALBITE	+	1.2353	
ANORTH	+	0.9935	
CHLORITE	+	0.0700	
CO2 GAS		0.5671	
GIBBSITE	-	-3.2177	
K-MONT	-	-0.0663	
RHODOCHR	-	-0.0084	
SiO2	-	-5.7064	
FERRIHYD	-	-0.0012	

This yielded 33 successful solutions of 11,440 models tested. Eleven of these were included in the most successful mix ratio of 1 part ground water from M4-05 with 1.21 parts water with the composition of background water (BKG-06); the most realistic of these is noted above. The precipitation of potassium montmorillonite, rhodochrosite, and ferrihydrite is required by the preferred solution. However, it is unlikely that montmorillonite can precipitate directly from solution, and rhodochrosite normally requires supersaturation and more reducing conditions. Therefore, none of the solutions appear realistic. All solutions in the favorable

mix ratio included albite, anorthite, chlorite, carbon dioxide, potassium montmorillonite, rhodochrosite, and ferrihydrite. There were no oversaturated trace metal precipitates predicted by WATEQ4F.

Conclusions

In the 50 years since the deposition of mill tailings at the study site ended, acidic conditions have developed, resulting in high concentrations of dissolved heavy metals and other contaminants in the tailings pore water. Physical observation of the solid samples collected during monitoring well drilling show, from top to bottom, zones of unsaturated tailings, saturated tailings, carbonaceous lake sediments grading into volcanic silts, colluvial gravel, and fractured bedrock. The lake sediments immediately below the tailings consist of 30 to 60 cm of organic-rich material intermixed with calcareous silts containing large amounts of snail shells. These below-tailings sediments may be instrumental in causing the geochemical behavior of released tailings pore water.

The transition from the vadose zone to the saturated zone in the tailings and the location of saturated lake sediments and silts below the tailings were verified by core samples and in situ moisture content and density depth profiles. These measurements were taken with a downhole neutron probe at eight locations in the tailings pile. Two of the neutron probe profiles showed layers of high moisture content and low density in the vadose zone about 46 cm below the surface. A 61-cm-long sample of one such layer showed a 2.5- to 5-cm-thick hardpan in the center of the sample. Tailings below the hardpan were much wetter, finer, and less oxidized than the tailings above. The hardpan appears to reduce and/or alter the downward flow of water and possibly acts as a barrier to atmospheric oxygen, impeding the pyrite oxidation process below. Concentrations of soluble metals in the pore water below the hardpan were considerably less than concentrations at similar depths in an area where no hardpan existed. In addition, grain-size comparisons between vadose and satu-

rated zone samples taken from well P3A showed 8 times more 0.01-mm particles in the saturated zone than in the vadose zone. This difference in grain-size distribution may be correlated to differences in water quality in the vadose and saturated zones at the site.

Potentiometric elevations in the tailings impoundment indicate the direction of the horizontal component of flow is toward the dam, at a gradient of about 5.6×10^{-3}. The low hydraulic gradient coupled with relatively low hydraulic conductivity (10^{-5}) of the tailings material implies extremely slow downgradient groundwater flow through the tailings. No measurements of vertical gradient in the saturated tailings exist. The direction of water that enters the tailings as meteoric water is downward. On the basis of a reduction in grain size (and presumably hydraulic conductivity) at the base of the tailings and a large reduction in soluble metal concentrations in the sediments just below the tailings, horizontal flow at the contact between the tailings and underlying sediments can be inferred. The vertical distribution of head in the sediments below the tailings shows a slight upward gradient in the spring, indicating the potential for upwelling in that zone and possibly into the base of the tailings during part of the year. From a positive environmental aspect, the decrease in hydraulic conductivity and a low gradient through and across the tailings appears to result in a slow and naturally controlled release of soluble metals from the tailings into the colluvium. However, the long periods over which the pore water is in contact with the tailings also results in long-term mechanical weathering and chemical reactivity. Once the tailings pore water enters the colluvium, the apparent increase in gradient may allow dispersion and mixing, and the increase in pH may allow chemical precipitation.

Long-term water quality monitoring at the field study site indicates that the saturated pore water in the tailings has generally higher concentrations of metals than pore water in the vadose zone, although the vadose water is more acidic and has more oxidation potential. Contaminants in solution migrate into the saturated zone. The sediments below the tailings are rich in calcium carbonate from snail shells, which may aid in neutralizing the acidic pore water. As the tailings pore water discharges to the colluvium, many events occur that affect contaminant flow and degree of metal concentration downgradient. These include hydrogeochemical reactions, dilution, advection, and dispersion. At a distance of 550 m downgradient from the impoundment, all measured dissolved constituents, except Ca, Mg, Mn, Na, and S, naturally attenuate to near background concentrations.

The hydrogeochemical computer models certainly support the commonly accepted belief that dissolution results from oxidation in the vadose zone. There are two potentially dominant attenuation mechanisms active immediately beneath and downgradient from the impoundment: oxidation or neutralization with minor oxidation. Both are supplemented by mixing with background water. Additional information is needed to identify which is occurring. Because almost no secondary minerals are predicted to be oversaturated in the entire system, even though trace metal attenuation is rapid, their coprecipitation with Fe and Mn minerals is very probable, with exchange and sorption likely playing a lesser role.

The basic chemical mechanisms active at sulfidic mine waste sites tend to be generally universal. However, the dominance of specific mechanisms or combinations of mechanisms is very site specific. Therefore, the results of this study are not directly transferable to all sites.

References

Ball, J. W. and D. K. Nordstrom. 1991. User's Manual for WATEQ4F, with revised thermodynamic data base and test cases for calculating speciation of major, trace and redox elements in natural water. U.S. Geol. Surv. Open File Report 91-183, 188 pp.

Blowes, D. W., J. A. Cherry and E. J. Reardon. 1987. The hydrogeochemistry of four inactive tailings impoundments: Perspectives on tailings pore water evolution. Proc., 1987 Natl. Symp. on Min., Hydrology, Sedimentology, and Reclamation (Dec. 7-11, 1987, Univ. KY, Lexington, KY), pp. 253-261.

Boorman, R. S. and D. M. Watson. 1976. Chemical processes in abandoned sulphide tailings dumps and environmental implication for northeastern New Brunswick. Can. Min. and Metall. Bull., v. 69:86-96.

Lambeth, R. H. 1992. Hydrogeochemical characteristics of an unconsolidated aquifer downgradient from an oxidized, sulfidic mine tailings impoundment. M.S. thesis, E. WA Univ., Cheney, WA, 140 pp.

Parkhurst, D. L., L. N. Plummer and D. C. Thorstenson. 1982. BALANCE - A computer program for calculating mass transfer for geochemical reactions in ground water. U.S. Geol. Surv. Water Resource Investigation 82-14, 29 pp.

Sill, W. R. and K. J. Sjostrom. 1990. A geophysical investigation to determine groundwater velocities at a site in west-central Washington. Final service agreement report to U.S. Bureau of Mines, 13 pp.

Stewart, B. M., R. H. Lambeth and B. C. Williams. 1990. Effects of pyritic tailings in an abandoned impoundment on downgradient ground water quality. Proc., Western Regional Symp. on Min. and Miner. Processing Wastes, Berkeley, CA, pp. 133-142.

Williams, B. C. 1992. Comparison of multivariate statistics and the geochemical code WATEQ4F for water quality interpretation in acidic tailings. Ph.D. dissertation, Univ. of ID, 164 pp.